



HHS Public Access

Author manuscript

ACS Appl Bio Mater. Author manuscript; available in PMC 2019 November 19.

Published in final edited form as:

ACS Appl Bio Mater. 2018 November 19; 1(5): 1430–1439. doi:10.1021/acsabm.8b00380.

Injectable Macroporous Hydrogel Formed by Enzymatic Cross-Linking of Gelatin Microgels

Shujie Hou, Rachel Lake, Shihwa Park, Seth Edwards, Chante Jones, Kyung Jae Jeong
Department of Chemical Engineering, University of New Hampshire, Durham, NH 03824

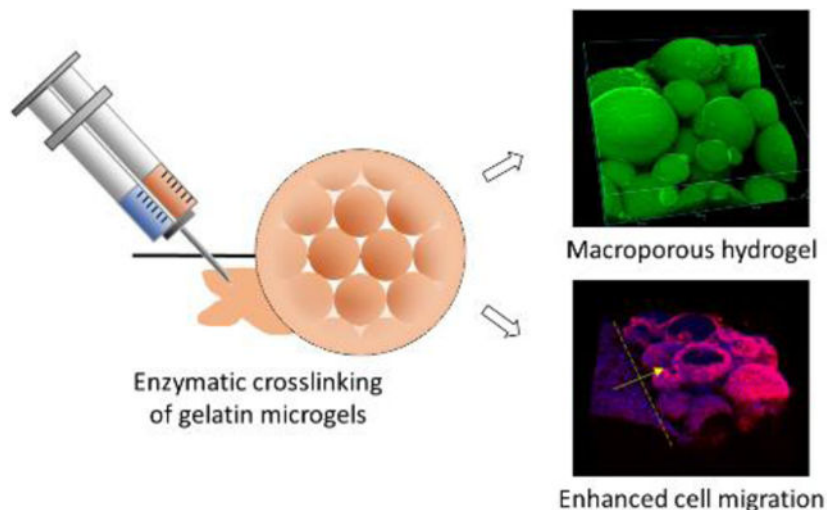
Abstract

Injectable hydrogels can be useful tools for facilitating wound healing since they conform to the irregular shapes of wounds, serving as a temporary matrix during the healing process. However, the lack of inherent pore structures of most injectable hydrogels prohibits desired interactions with the cells of the surrounding tissues limiting their clinical efficacy. Here, we introduce a simple, cost-effective and highly biofunctional injectable macroporous hydrogel made of gelatin microgels crosslinked by microbial transglutaminase (mTG). Pores are created by the interstitial space among the microgels. A water-in-oil emulsion technique was used to create gelatin microgels of an average size of 250 μ m in diameter. When crosslinked with mTG, the microgels adhered to each other to form a bulk hydrogel with inherent pores large enough for cell migration. The viscoelastic properties of the porous hydrogel were similar to those of nonporous gelatin hydrogel made by adding mTG to a homogeneous gelatin solution. The porous hydrogel supported higher cellular proliferation of human dermal fibroblasts (hDFs) than the nonporous hydrogel over two weeks, and allowed the migration of hDFs into the pores. Conversely, the hDFs were unable to permeate the surface of the nonporous hydrogel. To demonstrate its potential use in wound healing, the gelatin microgels were injected with mTG into a cut out section of an excised porcine cornea. Due to the action of mTG, the porous hydrogel stably adhered to the cornea tissue for two weeks. Confocal images showed that a large number of cells from the cornea tissue migrated into the interstitial space of the porous hydrogel. The porous hydrogel was also used for the controlled release of platelet-derived growth factor (PDGF), increasing the proliferation of hDFs compared to the nonporous hydrogel. This gelatin microgel-based porous hydrogel will be a useful tool for wound healing and tissue engineering.

Graphical Abstract

*Corresponding author: Kyungjae.Jeong@unh.edu. Tel: (603) 862-1917.

SUPPORTING INFORMATION: gelatin microgels through 26G needle, optical micrograph of macroporous hydrogel, rheology data, hydrogel degradation rates, confocal images of the live/dead assay, 3D images of cornea-hydrogel interface, maximum intensity projection of confocal images, FITC-BSA-loaded microgels.



Keywords

injectable hydrogel; porous; wound healing; microgels; gelatin; mTG; controlled release

1. Introduction

Due to their hydrophilic nature, hydrogels generally absorb a large quantity of water¹, which makes them ideal materials to interface human tissues, such as in wound dressings^{2–5}, contact lens^{6–10}, drug delivery^{11–14}, and tissue engineering^{15–19}. Hydrogels can be made injectable through various in situ crosslinking mechanisms and conform to the irregular topography of the applied site²⁰. This makes hydrogels an attractive option for use in wound healing applications.

Wound healing is a complex cellular and biochemical process, typically involving inflammation, new tissue formation, and remodeling phases²¹. When the wound size exceeds a critical value, or when the patient has compromised health conditions such as diabetes, proper wound healing process is seriously impeded. Biodegradable hydrogels applied to wounds can serve as a temporary matrix to facilitate the wound healing process. One of the major challenges regarding injectable hydrogels for such applications is the lack of inherent macropores to allow the migration of cells from neighboring tissue since the gel is formed on the wound site directly from a continuous liquid phase. The typical mesh size of hydrogels is a few nanometers to a few tens of nanometers^{22–23}, which is orders of magnitude smaller than the dimension of cells ($\sim 10\mu\text{m}$).

A number of methods have been developed to make macroporous injectable hydrogels in order to enhance the hydrogels' ability to interact with surrounding cells. Hydrogels that are crosslinked in a frozen state can be thawed and made into a highly porous scaffold which can be injected through a needle and regain its original shape^{24–26}. However, the shape of the hydrogel must be pre-determined and it is a challenge to tailor the shape of the hydrogel to the wound site. Injectable hydrogels that are formed by crosslinking biocompatible polymers with enzyme-sensitive peptides can also enable the migration of cells within the

hydrogel through the cleavage of peptides by the cell-secreted enzymes, such as matrix metalloproteinases (MMPs)^{27–30}. Pores for cell migration are formed as the cells secrete MMPs and cleave the peptide crosslinkers. However, one drawback of this approach is that the mechanical integrity of the hydrogel can be compromised as its enzymatic degradation by the infiltrating cells progresses. Photocuring of gelatin-derived injectable hydrogels has been shown to result in inherent pore structures and to enhance wound healing³¹, but the pore size of such hydrogels is not large enough for rapid cell migration as can be demonstrated by the prolonged round morphologies of the cells when the cells are encapsulated in the hydrogel^{31–32}. Another approach of forming macropores within the hydrogels is by assembling microgels. This idea has been explored for regenerative medicine^{33–36} and tissue engineering^{37–40}. Recently, a novel injectable macroporous hydrogel using a microgel-assembly for accelerated wound healing was reported⁴¹. In this case, monodisperse polyethylene glycol (PEG) microgels were enzymatically crosslinked through cell adhesive peptides, creating macropores through the interstitial space among microgels. When applied to a rat skin wound model *in vivo*, this porous hydrogel induced more rapid cell migration and wound healing compared to the nonporous counterpart. Due to the inherent macropores, this formulation could also encapsulate cells in the pores and induce rapid cell spreading and proliferation within the hydrogel. However, this method requires a series of chemical modifications of synthetic materials to make the hydrogel bioactive and enzymatically curable.

In this research, we introduce an injectable macroporous hydrogel by annealing physically crosslinked gelatin microgels by an enzyme - microbial transglutaminase (mTG) (Fig 1). Gelatin is a natural protein derived from collagen, and various forms of gelatin hydrogels have been made for applications in wound healing in skin^{5, 42–44} or ocular tissues^{31, 45} due to its low cost and well-known bioactivity and biocompatibility. mTG creates covalent bonds between glutamine and lysine residues of gelatin, and forms covalent crosslinks between and within the gelatin microgels⁴⁶. Similar to annealed PEG microgels, pores for cell migration are created by the interstitial space among the gelatin microgels. However, unlike the PEG-based macroporous hydrogel, the gelatin-based macroporous hydrogel introduced herein displays inherent bioactivity for cell adhesion and proliferation without any chemical modifications of the raw materials, such as the use of cell adhesive peptides. We also demonstrate the macroporous hydrogel's capability of controlled release of growth factors, which makes this novel formulation even more promising for the applications in wound healing.

2. Materials and methods

All materials were purchased from Sigma-Aldrich (St. Louis, MO) unless specified. Microbial transglutaminase (mTG) was purchased from Ajinomoto (Fort Lee, NJ). Sterile phosphate buffer saline (PBS, pH 7.4) was purchased from Gibco (Carlsbad, CA). Dulbecco's Modified Eagle's Medium (DMEM), fetal bovine serum (FBS), penicillin/streptomycin, alamarBlue, actinRed 555, albumin-fluorescein isothiocyanate conjugate (FITC-BSA), and betadine were purchased from Invitrogen (Frederick, MD). The four-arm polyethylene glycol maleimide (20k) (PEG-MAL) was purchased from JenKem technology (Plano, TX). Human dermal fibroblasts (hDFs) were purchased from Lonza (Portsmouth,

NH). Platelet-derived growth factor BB (PDGF-BB) was purchased from Boster Bio (Pleasanton, CA). The fresh pig eyeballs were obtained from Frist Visiontech (Sunnyvale, Texas).

2.1. Microgel synthesis and mTG crosslinking

Gelatin microgel was prepared by the water-in-oil emulsion method described by Li et al.⁴⁷. Briefly, gelatin (Type 1, from bovine and porcine bones) was dissolved in 20 mL deionized water at 50–55 °C to make 10% (w/v) solution. The gelatin solution then was added dropwise to 200 mL olive oil at 50–55 °C and stirred for 1 hour. The temperature of the mixture was lowered to reach room temperature for 30 min with stirring. Then the mixture was placed in an ice–water bath for additional 30 min with stirring to solidify the microgels by inducing physical crosslinking. 100 mL of precooled acetone (4 °C) was added into the mixture to precipitate the microgels with stirring for 30 min in the ice–water bath. The microgels were separated from the olive oil and acetone through vacuum filtration and further washed twice with 60 mL of precooled acetone. The microgels were lyophilized and kept dry until use. mTG at 20% (w/v) concentration in PBS was mixed with 10% (w/v) gelatin microgel in PBS at 1:5 ratio to form a porous hydrogel, or mixed with 10% (w/v) gelatin solution in PBS at 1:5 ratio to form a non-porous hydrogel. The final concentration of mTG and gelatin was 3.3% and 8.3%, respectively.

2.2. Rheological characterization

The viscoelastic properties of the porous hydrogel and non-porous hydrogel were characterized with a rheometer (TA Instruments AR 550, New Castle, DE). Either gelatin microgel solution or plain gelatin solution was mixed with mTG and placed under a plane stainless steel geometry (diameter = 2cm). The linear viscoelastic regime was first determined by a stress sweep. The gelation kinetics was observed by the time sweep, with an oscillatory stress of 1 Pa at 10 rad/s and 37°C. Once the gelation was completed, the frequency sweep was performed between 0.1 and 100 rad/s with an oscillatory stress of 1 Pa at 37°C. For the temperature sweep, temperature was changed from 4°C to 45°C with an oscillatory stress of 1 Pa at 10 rad/s.

2.3. Characterization of the gelatin microgels and porous hydrogel

The microgels were visualized with an optical microscope (EVOS XL, Life Technologies, Carlsbad, CA), and scanning electron microscope (SEM) (Tescan Lyra3 GMU FIB SEM, Brno, Czech Republic). For SEM, the microgels were lyophilized and coated with gold/palladium to avoid charging. Size distribution of the microgels was obtained from the optical microscope and SEM images using ImageJ. After the porous hydrogel was formed, the detailed structure of the hydrogel was visualized with optical microscope, SEM, and confocal microscope (Nikon A1R HD, Melville, NY). For the SEM imaging, the hydrogel was dried by critical point drying. For the confocal microscopy, the porous hydrogel was formed from the microgels mixed with fluorescein isothiocyanate-labelled bovine serum albumin (FTIC-BSA) (0.1%).

2.4. Enzymatic degradation of hydrogels

The kinetics of the enzymatic degradation of porous and nonporous gelatin hydrogels was obtained by incubating the hydrogels in collagenase type II solution (concentration = 0.5 U/mL)⁴⁸. At different time points (0h, 4h, 24 h), the hydrogels were collected, lyophilized and weighed to calculate the amount of degraded gelatin.

2.5. Human dermal fibroblast (hDF) culture on the hydrogels

Human dermal fibroblasts (hDFs) were cultured in T75 flasks using Dulbecco's Modified Eagle Medium (DMEM) supplemented with 10% fetal bovine serum (FBS) and 1% penicillin/streptomycin (pen/strep). The culture was performed in a humidified chamber with 5% CO₂ at 37°C. Cells under passage 4 were used for all the experiments.

To test cellular proliferation on the hydrogels, the porous and non-porous hydrogels (600 µL) were formed in 24-well plates, followed by sterilization in 70% ethanol overnight. Human dermal fibroblasts (hDFs) were seeded on the hydrogel surface with the seeding density of 1×10^4 cells/cm². The media was changed twice a day. The proliferation of hDFs was measured by almarBlue on day 7 and 14 by measuring the fluorescence at 595 nm (excitation at 555 nm).

The three-dimensional distribution of hDFs in the hydrogels was visualized by confocal microscopy. After 14 days from the initial seeding, the samples were fixed in 4% formaldehyde in PBS overnight, and stained with actinRed 555 to stain the actin cytoskeleton of hDFs. The Z-section images were obtained using confocal microscope (Nikon A1R HD, Melville, NY) and 2D-projection, 3D images and cross-sectional images were obtained using ImageJ.

2.6. Application of the hydrogel to the porcine cornea tissues

Fresh pig eyeballs were sterilized by immersion in povidone-iodine and rinsing several times with sterile PBS. Cornea tissues were collected from the eyeballs using surgical scissors. A hole was created in the middle of the cornea using a biopsy punch (8 mm in diameter). The hole in the cornea was filled by injecting either gelatin microgel solution or plain gelatin solution with mTG to create porous or non-porous hydrogel, respectively. The assembly was incubated for 1 hour at 37°C for curing, after which DMEM supplemented with FBS and pen/strep was added. The tissue-hydrogel assembly was fed daily for 14 days before fixation in formaldehyde. The corneas were stained with actinRed555 and DAPI and imaged by confocal microscope.

2.7. Controlled release of FITC-BSA and platelet-derived growth factor (PDGF)

In order to understand the nature of protein loading in the porous hydrogel, the microgels were incubated in a FITC-BSA solution (100 µg/mL) for 48 hours at room temperature. After the supernatant was removed, the distribution of FITC-BSA within the microgels was visualized with a confocal microscope.

PDGF loading into the microgels was achieved using the same method except that the concentration of PDGF was reduced to 20 µg/mL. A PDGF-loaded porous hydrogel was

formed by mixing these microgels with unloaded gelatin microgels at 1:9 ratio (v:v) and crosslinking it using mTG. PDGF-loaded non-porous hydrogel was created by adding PDGF to a gelatin solution, which was crosslinked by mTG. After the hydrogels were formed, the release of PDGF was measured at day 1, 2, 3, 7 and 14 by enzyme-linked immunosorbent assay (ELISA).

2.8. hDF proliferation with the controlled release of PDGF from the hydrogels

hDFs were seeded on the 24 well plates with the seeding density of 1500 cells/cm². On day 2, PDGF-loaded porous and nonporous hydrogels were added to the cell culture through the transwell inserts with semi-permeable membranes. The proliferation of hDFs was measured by almarBlue assay on day 7.

2.9. Statistics

The data are presented as means \pm standard deviation unless stated otherwise. The statistical significance of the difference among multiple sample groups was tested by ANOVA followed by Tukey's *post hoc* test using Origin 8.1.

3. Results and Discussion

3.1. Characterization of gelatin microgels

The microgels were synthesized by the water-in-oil emulsion method. The size distribution of the dry microgels were measured by SEM images after lyophilization. The microgels were spherical in shape (Fig 2a) and polydisperse with the average diameter of 63 μ m (Fig 2b). When the microgels were dispersed in water, they swelled significantly (Fig 2c) to an average diameter of 253 μ m (Fig 2d). The swelling ratio was 14.7. At 10% (w/v) concentration and at 37°C, gelatin microgels formed a viscous solution, making them injectable through a gauge 26 needle (Fig S1).

3.2. Formation and characterization of the macroporous hydrogel.

A bulk macroporous hydrogel was formed by annealing the gelatin microgels with mTG. When mixed with mTG, the microgel solution became more viscous over time (< 5 min) and eventually became a bulk gel. When viewed under the optical microscope, the assembly of spherical microgels within the hydrogel was evident (Fig S2). The SEM image clearly demonstrates a three-dimensional network of spherical microgels with void space between microgels (Fig 3a). Confocal microscope images of the hydrogel further confirmed these findings (Fig 3b). The pore size was mostly in the range of tens of microns, which is large enough for cell migration⁴⁹. The porosity of the hydrogel was estimated to be 0.43 by the confocal microscope images. This value is in good agreement with the void fraction of random packing of spheres, which is around ~0.4 for various sphere size distributions and materials⁵⁰.

Viscoelastic properties of the hydrogels were characterized to understand the nature of the crosslinks created by mTG (Fig 4, Fig S3). The time-sweep measurements show the kinetics of the covalent crosslinking by mTG. Both G' and G'' of the porous hydrogel (gelatin microgel + mTG) at t = 0 were higher than the nonporous hydrogel (gelatin solution + mTG)

because of the following two reasons: (i) Data collection for the porous hydrogel was more delayed than for the nonporous hydrogel (~3 min) due to the longer sample preparation time. (ii) In addition, gelatin concentration in the microgels was higher than that of the bulk gelatin solution because there was void space within the microgel solution even though its weight per volume concentration was the same (10%) as the bulk gelatin solution. In another recent study, the inclusion of gelatin microgels in a covalently crosslinked PEG hydrogel also resulted in a much higher initial G' and G'' in a time sweep⁴⁷, although direct comparisons are difficult to be made due to the differences in the overall hydrogel structures. However, the final G' values after 1 hour were comparable to each other (Fig 4a). G' of the microgels without mTG remained unchanged due to the lack of chemical crosslinking, indicating the microgels alone without crosslinking by mTG do not form a bulk hydrogel.

Once the gelation was completed, G' was measured as a function of temperature (Fig 4b). The temperature-sweep measurements provide more information about the nature of crosslinks. As temperature decreased, G' increased for both porous and nonporous hydrogels due to the formation of physical crosslinks by hydrogen bonding. G' of gelatin microgels without mTG also increased for the same reason. As the temperature increased, the physical crosslinks were weakened resulting in a continuous decrease in G' for both the porous and nonporous hydrogels. This trend continued until ~30°C at which G' reached a plateau at ~3000 Pa. This is attributed to the presence of the covalent bonds created by the actions of mTG because covalent crosslinks by amide bonds in this temperature regime are stable. The fact that G' of the porous hydrogel is comparable to that of the nonporous hydrogel indicates that the chemical crosslinking by mTG occurred within the microgels as well as between microgels. In comparison, G' of microgels without mTG decreased until the microgels completely melted. The frequency sweep further confirmed that the viscoelastic properties of the porous hydrogel are similar to the nonporous hydrogel (Fig S3). The slight increase of G' as a function of frequency is a characteristic of the hydrogels that are crosslinked both physically and chemically⁵¹.

3.3. Enzymatic degradation of the porous hydrogel.

It is essential that a hydrogel added to a wound is able to degrade over the course of the wound healing process. Gelatin can be degraded by many cell-secreted enzymes, such as collagenases and gelatinases^{52–53}. When incubated in collagenase type II solution, the porous gelatin hydrogel degraded slightly slower than the nonporous hydrogel than the nonporous hydrogel (82% degradation for porous hydrogel vs 93% degradation for nonporous hydrogel at 24 hour) (Fig S4). However, there was no statistical significance of the difference ($p = 0.198$ at 4 hours and 0.086 at 24 hours). This result indicates that the porous gelatin hydrogel can serve as a temporary matrix during the wound healing process.

3.4. In vitro culture of human dermal fibroblasts (hDFs) on the hydrogels.

Bioactivity of the macroporous hydrogel was compared to the nonporous hydrogel by seeding hDFs on the surface of the hydrogels and monitoring cell proliferation over two weeks using alamarBlue assay (Fig 5). Proliferation of hDFs on the porous hydrogel was higher than on the nonporous hydrogel over the two-week period, and there was no statistical significance between the two groups at week 2. Various studies have shown that

mTG-crosslinked nonporous gelatin hydrogel supports cell adhesion and proliferation^{54–55}. The fact that the macroporous gelatin hydrogel resulted in a higher cellular proliferation than the nonporous gelatin hydrogel proves its excellent bioactivity properties and its potential use in biological systems such as for wound healing. The excellent hDF proliferation on the gelatin macroporous hydrogel is comparable to the PEG-based macroporous hydrogel, which also supported robust proliferation of hDFs encapsulated in the hydrogel⁴¹. The advantage of using gelatin as a base material for the injectable macroporous hydrogel as opposed to other synthetic polymers is highlighted by comparing the proliferation of hDF on nonporous PEG hydrogel created by crosslinking maleimide functionalized 4-arm polyethylene glycol (20kDa) by dithiothreitol. Hydrogels made of synthetic polymers typically do not support cell adhesion or proliferation without chemical modifications with bioactive moieties, such as cell adhesive RGD peptides^{56–58}. In contrast, the gelatin-based injectable porous hydrogel does not require any chemical modifications to promote cell adhesion and proliferation because of innate cell adhesive ligands, such as RGD, present in gelatin. The live/dead assay showed that the cells in both porous and nonporous hydrogels were viable (Fig S5).

When the hDFs were stained for actin cytoskeleton and visualized by confocal microscopy, some hDFs were found to grow beyond the first layer of the microgels despite the fact that all cells were initially added on the hydrogel surface (Fig 6a). This shows that the gelatin macroporous hydrogel not only supports cell adhesion and proliferation, but also allows cell migration through the pores. This is an important feature of the macroporous hydrogel because cell migration is an essential phenomenon during the wound healing process. In contrast, the cells on the nonporous gelatin hydrogel grew exclusively on the surface of the hydrogel (Fig 6b). Due to the small polymer mesh size, the hydrogel must be degraded first for the cell migration into the nonporous hydrogel⁴⁷, which was not observed during the time frame of our study.

3.5. Application of the macroporous hydrogel to the porcine cornea *ex vivo*.

To test the feasibility of using this injectable porous hydrogel in facilitating cell migration and wound healing in a damaged tissue, we applied the hydrogel (without cells) to a freshly cut porcine cornea tissue. A small hole (8mm in diameter) was punctured in the middle of the cornea and the gelatin microgel solution or gelatin solution was injected into the hole with mTG to form a porous or nonporous hydrogel. The hydrogel stably adhered to the tissue through the action of mTG during the two weeks' span of tissue culture (Fig 7a, b). On day 0, cells were found only in the cornea tissue as no cells were present in the hydrogels (Fig 7c, d). On day 14, the hydrogel phase was densely populated by the cells, mainly the corneal epithelial cells, that migrated from the cornea tissue (Fig 7e, f, Fig S6, Fig S7). As in the *in vitro* culture of hDFs, cells were found not only on the hydrogel surface but also inside the void space of the porous hydrogel, whereas migrated cells were found exclusively on the surface of the nonporous hydrogel (Fig S8). The live/dead assay showed that the majority of the cells in the cornea tissue and the hydrogels (both porous and nonporous) were viable (Fig S9).

It should be noted that the current form of porous gelatin hydrogel can only be used for small-sized peripheral corneal wounds due to its low transmittance in the visible range (~ 30 %). In this study, porcine cornea was chosen as a model tissue for their ready accessibility and ease of tissue culture^{59–60}. Considering the necessity of porous structure for the facilitated cell migration and wound healing⁴¹, our results point to the potential of this porous hydrogel formulation being used to facilitate the wound healing process in non-ocular tissues (e.g. skin) as well by allowing cell migration and proliferation within the hydrogel.

Another limitation of the current formulation for the clinical applications is a relatively slow curing time by mTG (~ 30 min). Potential solutions to address this issue are (i) the use of a composite material between gelatin and alginate⁶¹ for microgels, which can be rapidly crosslinked by calcium, followed by the covalent crosslinking by mTG, and (ii) the incorporation of photocurable gelatin (e.g. methacrylated gelatin⁶²) in the microgels followed by UV crosslinking.

3.6. Controlled release of platelet-derived growth factor (PDGF) from the macroporous hydrogel.

Various growth factors play essential roles during the wound healing process. For example, platelet-derived growth factor (PDGF) is released during wound healing and induces the proliferation of fibroblasts for the secretion of a new extracellular matrix (ECM)^{63–65}. An ideal hydrogel formulation to facilitate wound healing, therefore, should have the capability of controlled release of growth factors.

Hydrogels are ideal materials for the controlled release of protein drugs^{11, 66–67} because the hydrated environment of the hydrogels allows the proteins to maintain their native 3D structures and functions⁶⁸. For the characterization of the nature of protein loading in the gelatin microgels, the gelatin microgels were incubated with FITC-labeled bovine serum albumin (FITC-BSA) for 48 hours to induce diffusion-driven loading of the protein in the microgels. The proteins were found mainly on the surface of the microgels as the diffusion of the protein occurred through the surface (Fig S10).

Human PDGF was loaded in the microgels in the same way as FITC-BSA. The PDGF-loaded microgels were crosslinked by mTG to form a PDGF-loaded macroporous hydrogel. PDGF was loaded in the nonporous hydrogel by mixing PDGF with the gelatin solution before crosslinking with mTG. For both hydrogels, the overall release of PDGF was inefficient over two weeks (13% and 9% release of the initial loading from the porous and nonporous hydrogel, respectively) (Fig 8). The reason for such inefficient release is likely due to covalent immobilization of PDGF to the hydrogels by the action of mTG during the crosslinking process. Covalent attachment of proteins within the hydrogel during the crosslinking process is common for the covalently crosslinked injectable hydrogels⁶⁹. It is also known that the positively charged growth factors are strongly bound to the negatively charged gelatin hydrogels, making the growth factor release inefficient even if the loading is performed after the covalent crosslinking of the hydrogel⁷⁰. Nonetheless, the porous hydrogel released a higher amount of PDGF at a steadier rate than the nonporous hydrogel. Considering that the gelatin hydrogels degrade in the presence of collagenases and there

exist various kinds of collagenases and gelatinases *in vivo*⁷¹, we expect that the growth factor release from the gelatin hydrogels will be more efficient *in vivo* with the degradation of the hydrogel⁷².

When the PDGF was released into the culture medium of hDFs for two weeks through semi-permeable membranes (Fig 9a,b), the cellular proliferation increased by 1.3 times for the porous hydrogel when compared to the culture without PDGF (Fig 9c) ($p = 0.039$). No significant differences were observed at earlier time points. PDGF release from the nonporous hydrogel also increased the proliferation of hDFs, but there was no statistical significance compared to the culture without PDGF ($p = 0.900$).

4. Conclusion

Addition of mTG to gelatin microgels induced covalent crosslinks within and between microgels, forming a bulk network of macroporous hydrogel. This injectable hydrogel did not require any chemical modification before the gelation. The hydrogel was noncytotoxic to hDFs and allowed adhesion and proliferation of hDFs on the hydrogel surface and cell migration into the hydrogel pores. Upon injection into a hole in porcine corneal tissue, a large number of cells from the surrounding cornea tissue migrated to the porous hydrogel and proliferated both on the surface and in the pores of the hydrogel. Controlled release of PDGF over two weeks was achieved using this hydrogel, which enhanced the proliferation of hDFs. Although we did not show the facilitated wound healing *in vivo*, the fact that this simple and low-cost hydrogel allows the cellular adhesion and migration into the porous structure indicates its potential applications in wound healing and tissue engineering.

Supplementary Material

Refer to Web version on PubMed Central for supplementary material.

ACKNOWLEDGMENTS

This work was supported in part by an NIH COBRE Center of Integrated Biomedical and Bioengineering Research (CIBBR, P20 GM113131) through an Institutional Development Award (IDeA) from the National Institute of General Medical Sciences.

References

1. Maitra J; Shukla VK, Cross-Linking in Hydrogels-a Review. *Am. J. Polym. Sci* 2014, 4 (2), 25–31.
2. Zhao X; Wu H; Guo B; Dong R; Qiu Y; Ma PX, Antibacterial Anti-Oxidant Electroactive Injectable Hydrogel as Self-Healing Wound Dressing with Hemostasis and Adhesiveness for Cutaneous Wound Healing. *Biomaterials* 2017, 122, 34–47. [PubMed: 28107663]
3. Xu J; Tam M; Samaei S; Lerouge S; Barralet J; Stevenson MM; Cerruti M, Mucoadhesive Chitosan Hydrogels as Rectal Drug Delivery Vessels to Treat Ulcerative Colitis. *Acta Biomater.* 2017, 48, 247–257. [PubMed: 27769943]
4. Tavakoli J; Mirzaei S; Tang Y, Cost-Effective Double-Layer Hydrogel Composites for Wound Dressing Applications. *Polymers* 2018, 10 (3), 305.
5. Balakrishnan B; Mohanty M; Umashankar P; Jayakrishnan A, Evaluation of an *in Situ* Forming Hydrogel Wound Dressing Based on Oxidized Alginate and Gelatin. *Biomaterials* 2005, 26 (32), 6335–6342. [PubMed: 15919113]

6. Schroeder TB; Guha A; Lamoureux A; VanRenterghem G; Sept D; Shtein M; Yang J; Mayer M, An Electric-Eel-Inspired Soft Power Source from Stacked Hydrogels. *Nature* 2017, 552 (7684), 214. [PubMed: 29239354]
7. Horne RR; Judd KE; Pitt WG, Rapid Loading and Prolonged Release of Latanoprost from a Silicone Hydrogel Contact Lens. *J. Drug Deliv. Sci. Technol* 2017, 41, 410–418.
8. Nicolson PC; Vogt J, Soft Contact Lens Polymers: An Evolution. *Biomaterials* 2001, 22 (24), 3273–3283. [PubMed: 11700799]
9. Ciolino JB; Stefanescu CF; Ross AE; Salvador-Culla B; Cortez P; Ford EM; Wymbs KA; Sprague SL; Mascoop DR; Rudina SS; Trauger SA; Cade F; Kohane DS, In Vivo Performance of a Drug-Eluting Contact Lens to Treat Glaucoma for a Month. *Biomaterials* 2014, 35 (1), 432–439. [PubMed: 24094935]
10. Ciolino JB; Hoare TR; Iwata NG; Behlau I; Dohlman CH; Langer R; Kohane DS, A Drug-Eluting Contact Lens. *Invest. Ophthalmol. Visual Sci* 2009, 50 (7), 3346–3352. [PubMed: 19136709]
11. Yamamoto M; Ikada Y; Tabata Y, Controlled Release of Growth Factors Based on Biodegradation of Gelatin Hydrogel. *J. Biomater. Sci., Polym. Ed* 2001, 12 (1), 77–88. [PubMed: 11334191]
12. Cai S; Liu Y; Zheng Shu X; Prestwich GD, Injectable Glycosaminoglycan Hydrogels for Controlled Release of Human Basic Fibroblast Growth Factor. *Biomaterials* 2005, 26 (30), 6054–6067. [PubMed: 15958243]
13. Koutsopoulos S; Unsworth LD; Nagai Y; Zhang S, Controlled Release of Functional Proteins through Designer Self-Assembling Peptide Nanofiber Hydrogel Scaffold. *Proc. Natl. Acad. Sci. USA* 2009, 106 (12), 4623–4628. [PubMed: 19273853]
14. Zhang Y; Tao L; Li S; Wei Y, Synthesis of Multiresponsive and Dynamic Chitosan-Based Hydrogels for Controlled Release of Bioactive Molecules. *Biomacromolecules* 2011, 12 (8), 2894–2901. [PubMed: 21699141]
15. Tan H; Chu CR; Payne KA; Marra KG, Injectable in Situ Forming Biodegradable Chitosan-Hyaluronic Acid Based Hydrogels for Cartilage Tissue Engineering. *Biomaterials* 2009, 30 (13), 2499–2506. [PubMed: 19167750]
16. Rafat M; Li F; Fagerholm P; Lagali NS; Watsky MA; Munger R; Matsuura T; Griffith M, PEG-Stabilized Carbodiimide Crosslinked Collagen-Chitosan Hydrogels for Corneal Tissue Engineering. *Biomaterials* 2008, 29 (29), 3960–3972. [PubMed: 18639928]
17. Eke G; Mangir N; Hasirci N; MacNeil S; Hasirci V, Development of a Uv Crosslinked Biodegradable Hydrogel Containing Adipose Derived Stem Cells to Promote Vascularization for Skin Wounds and Tissue Engineering. *Biomaterials* 2017, 129, 188–198. [PubMed: 28343005]
18. Xavier JR; Thakur T; Desai P; Jaiswal MK; Sears N; Cosgriff-Hernandez E; Kaunas R; Gaharwar AK, Bioactive Nanoengineered Hydrogels for Bone Tissue Engineering: A Growth-Factor-Free Approach. *ACS Nano* 2015, 9 (3), 3109–3118. [PubMed: 25674809]
19. Van Vlierberghe S; Dubruel P; Schacht E, Biopolymer-Based Hydrogels as Scaffolds for Tissue Engineering Applications: A Review. *Biomacromolecules* 2011, 12 (5), 1387–1408. [PubMed: 21388145]
20. Ruel-Gariepy E; Leroux J-C, In Situ-Forming Hydrogels—Review of Temperature-Sensitive Systems. *Eur. J. Pharm. Biopharm* 2004, 58 (2), 409–426. [PubMed: 15296964]
21. Gurtner GC; Werner S; Barrandon Y; Longaker MT, Wound Repair and Regeneration. *Nature* 2008, 453 (7193), 314. [PubMed: 18480812]
22. Canal T; Peppas NA, Correlation between Mesh Size and Equilibrium Degree of Swelling of Polymeric Networks. *J. Biomed. Mater. Res* 1989, 23 (10), 1183–1193. [PubMed: 2808463]
23. Zustiak SP; Leach JB, Hydrolytically Degradable Poly (Ethylene Glycol) Hydrogel Scaffolds with Tunable Degradation and Mechanical Properties. *Biomacromolecules* 2010, 11 (5), 1348–1357. [PubMed: 20355705]
24. Bencherif SA; Sands RW; Bhatta D; Arany P; Verbeke CS; Edwards DA; Mooney DJ, Injectable Preformed Scaffolds with Shape-Memory Properties. *Proc. Natl. Acad. Sci. USA* 2012, 109 (48), 19590–19595. [PubMed: 23150549]
25. Koshy ST; Ferrante TC; Lewin SA; Mooney DJ, Injectable, Porous, and Cell-Responsive Gelatin Cryogels. *Biomaterials* 2014, 35 (8), 2477–2487. [PubMed: 24345735]

26. Koshy ST; Zhang DK; Grolman JM; Stafford AG; Mooney DJ, Injectable Nanocomposite Cryogels for Versatile Protein Drug Delivery. *Acta Biomater.* 2018, 65, 36–43. [PubMed: 29128539]
27. Lutolf MP; Lauer-Fields JL; Schmoekel HG; Metters AT; Weber FE; Fields GB; Hubbell JA, Synthetic Matrix Metalloproteinase-Sensitive Hydrogels for the Conduction of Tissue Regeneration: Engineering Cell-Invasion Characteristics. *Proc. Natl. Acad. Sci. USA* 2003, 100 (9), 5413–5418. [PubMed: 12686696]
28. Patterson J; Hubbell JA, Enhanced Proteolytic Degradation of Molecularly Engineered PEG Hydrogels in Response to Mmp-1 and Mmp-2. *Biomaterials* 2010, 31 (30), 7836–7845. [PubMed: 20667588]
29. Schultz KM; Kyburz KA; Anseth KS, Measuring Dynamic Cell-Material Interactions and Remodeling During 3d Human Mesenchymal Stem Cell Migration in Hydrogels. *Proc. Natl. Acad. Sci. USA* 2015, 112 (29), E3757–3764. [PubMed: 26150508]
30. Raeber G; Lutolf M; Hubbell J, Molecularly Engineered PEG Hydrogels: A Novel Model System for Proteolytically Mediated Cell Migration. *Biophys. J* 2005, 89 (2), 1374–1388. [PubMed: 15923238]
31. Li L; Lu C; Wang L; Chen M; White J; Hao X; McLean KM; Chen H; Hughes TC, Gelatin-Based Photocurable Hydrogels for Corneal Wound Repair. *ACS Appl. Mater. Interfaces* 2018, 10 (16), 13283–13292. [PubMed: 29620862]
32. Benton JA; DeForest CA; Vivekanandan V; Anseth KS, Photocrosslinking of Gelatin Macromers to Synthesize Porous Hydrogels That Promote Valvular Interstitial Cell Function. *Tissue Engineering Part A* 2009, 15 (11), 3221–3230. [PubMed: 19374488]
33. McGuigan AP; Sefton MV, Modular Tissue Engineering: Fabrication of a Gelatin-Based Construct. *J. Tissue Eng. Regen. Med* 2007, 1 (2), 136–145.
34. Du Y; Lo E; Ali S; Khademhosseini A, Directed Assembly of Cell-Laden Microgels for Fabrication of 3d Tissue Constructs. *Proc. Natl. Acad. Sci. USA* 2008, 105 (28), 9522–9527. [PubMed: 18599452]
35. Xu F; Wu C. a. M.; Rengarajan V; Finley TD; Keles HO; Sung Y; Li B; Gurkan UA; Demirci U, Three-Dimensional Magnetic Assembly of Microscale Hydrogels. *Adv Mater.* 2011, 23 (37), 4254–4260. [PubMed: 21830240]
36. Qi H; Ghodousi M; Du Y; Grun C; Bae H; Yin P; Khademhosseini A, DNA-Directed Self-Assembly of Shape-Controlled Hydrogels. *Nat. Commun* 2013, 4, 2275. [PubMed: 24013352]
37. Roam JL; Yan Y; Nguyen PK; Kinstlinger IS; Leuchter MK; Hunter DA; Wood MD; Elbert DL, A Modular, Plasmin-Sensitive, Clickable Poly (Ethylene Glycol)-Heparin-Laminin Microsphere System for Establishing Growth Factor Gradients in Nerve Guidance Conduits. *Biomaterials* 2015, 72, 112–124. [PubMed: 26352518]
38. Zhou W; Stukel JM; Cebull HL; Willits RK, Tuning the Mechanical Properties of Poly (Ethylene Glycol) Microgel-Based Scaffolds to Increase 3d Schwann Cell Proliferation. *Macromol. Biosci* 2016, 16 (4), 535–544. [PubMed: 26726886]
39. Xin S; Wyman OM; Alge DL, Assembly of PEG Microgels into Porous Cell-Instructive 3d Scaffolds Via Thiol-Ene Click Chemistry. *Adv. Healthcare Mater* 2018, 7 (11), e1800160.
40. Zhou W; Stukel JM; AlNiemi A; Willits RK, Novel Microgel-Based Scaffolds to Study the Effect of Degradability on Human Dermal Fibroblasts. *Biomed. Mater. (Bristol, U. K.)* 2018, 13 (5), 055007.
41. Griffin DR; Weaver WM; Scumpia PO; Di Carlo D; Segura T, Accelerated Wound Healing by Injectable Microporous Gel Scaffolds Assembled from Annealed Building Blocks. *Nat. Mater* 2015, 14 (7), 737. [PubMed: 26030305]
42. Zheng Y; Liang Y; Zhang D; Sun X; Liang L; Li J; Liu Y-N, Gelatin-Based Hydrogels Blended with Gellan as an Injectable Wound Dressing. *ACS Omega* 2018, 3 (5), 4766–4775. [PubMed: 30023901]
43. Zhao X; Sun X; Yildirimer L; Lang Q; Lin ZYW; Zheng R; Zhang Y; Cui W; Annabi N; Khademhosseini A, Cell Infiltrative Hydrogel Fibrous Scaffolds for Accelerated Wound Healing. *Acta Biomater.* 2017, 49, 66–77. [PubMed: 27826004]

44. Zhao X; Lang Q; Yildirim L; Lin ZY; Cui W; Annabi N; Ng KW; Dokmeci MR; Ghaemmaghami AM; Khademhosseini A, Photocrosslinkable Gelatin Hydrogel for Epidermal Tissue Engineering. *Adv. Healthcare Mater* 2016, 5 (1), 108–118.
45. Mimura T; Amano S; Yokoo S; Uchida S; Yamagami S; Usui T; Kimura Y; Tabata Y, Tissue Engineering of Corneal Stroma with Rabbit Fibroblast Precursors and Gelatin Hydrogels. *Mol. Vision* 2008, 14, 1819.
46. Yung C; Wu L; Tullman J; Payne G; Bentley W; Barbari T, Transglutaminase Crosslinked Gelatin as a Tissue Engineering Scaffold. *J. Biomed. Mater. Res., Part A* 2007, 83 (4), 1039–1046.
47. Li Y; Meng H; Liu Y; Narkar A; Lee BP, Gelatin Microgel Incorporated Poly (Ethylene Glycol)-Based Bioadhesive with Enhanced Adhesive Property and Bioactivity. *ACS Appl. Mater. Interfaces* 2016, 8 (19), 11980–11989. [PubMed: 27111631]
48. Shin SR; Aghaei-Ghareh-Bolagh B; Dang TT; Topkaya SN; Gao X; Yang SY; Jung SM; Oh JH; Dokmeci MR; Tang X, Cell-Laden Microengineered and Mechanically Tunable Hybrid Hydrogels of Gelatin and Graphene Oxide. *Adv Mater.* 2013, 25 (44), 6385–6391. [PubMed: 23996513]
49. Murphy CM; Haugh MG; O'Brien FJ, The Effect of Mean Pore Size on Cell Attachment, Proliferation and Migration in Collagen–Glycosaminoglycan Scaffolds for Bone Tissue Engineering. *Biomaterials* 2010, 31 (3), 461–466. [PubMed: 19819008]
50. Scott G; Kilgour D, The Density of Random Close Packing of Spheres. *J. Phys. D: Appl. Phys* 1969, 2 (6), 863.
51. Jeong KJ; Panitch A, Interplay between Covalent and Physical Interactions within Environment Sensitive Hydrogels. *Biomacromolecules* 2009, 10 (5), 1090–1099. [PubMed: 19301930]
52. Bányai L; Tordai H; Patthy L, Structure and Domain-Domain Interactions of the Gelatin-Binding Site of Human 72-Kilodalton Type Iv Collagenase (Gelatinase a, Matrix Metalloproteinase 2). *J. Biol. Chem* 1996, 271 (20), 12003–12008. [PubMed: 8662603]
53. Mladenovska K; Kumbaradzi E; Dodov G; Makraduli L; Goracinova K, Biodegradation and Drug Release Studies of Bsa Loaded Gelatin Microspheres. *Int. J. Pharm* 2002, 242 (1–2), 247–249. [PubMed: 12176256]
54. Maddaus A; Curley P; Griswold MA; Costa BD; Hou S; Jeong KJ; Song E; Deravi LF, Design and Fabrication of Bio-Hybrid Materials Using Inkjet Printing. *Biointerphases* 2016, 11 (4), 041002.
55. Yang G; Xiao Z; Long H; Ma K; Zhang J; Ren X; Zhang J, Assessment of the Characteristics and Biocompatibility of Gelatin Sponge Scaffolds Prepared by Various Crosslinking Methods. *Sci. Rep* 2018, 8 (1), 1616. [PubMed: 29371676]
56. Burdick JA; Anseth KS, Photoencapsulation of Osteoblasts in Injectable RGD-Modified PEG Hydrogels for Bone Tissue Engineering. *Biomaterials* 2002, 23 (22), 4315–4323. [PubMed: 12219821]
57. Groll J; Fiedler J; Engelhard E; Ameringer T; Tugulu S; Klok HA; Brenner RE; Moeller M, A Novel Star PEG-Derived Surface Coating for Specific Cell Adhesion. *J. Biomed. Mater. Res., Part A* 2005, 74 (4), 607–617.
58. Weber LM; Hayda KN; Haskins K; Anseth KS, The Effects of Cell-Matrix Interactions on Encapsulated Beta-Cell Function within Hydrogels Functionalized with Matrix-Derived Adhesive Peptides. *Biomaterials* 2007, 28 (19), 3004–3011. [PubMed: 17391752]
59. Salvador-Culla B; Jeong KJ; Kolovou PE; Chiang HH; Chodosh J; Dohlman CH; Kohane DS, Titanium Coating of the Boston Keratoprosthesis. *Transl Vis Sci Techn* 2016, 5 (2), 17.
60. Wang L; Jeong KJ; Chiang HH; Zurakowski D; Behlau I; Chodosh J; Dohlman CH; Langer R; Kohane DS, Hydroxyapatite for Keratoprosthesis Biointegration. *Invest. Ophthalmol. Visual Sci* 2011, 52 (10), 7392–7399. [PubMed: 21849419]
61. Wen C; Lu L; Li X, Mechanically Robust Gelatin–alginate Hydrogels by a Combination of Enzymatic and Ionic Crosslinking Approaches. *Macromolecular Materials and Engineering* 2014, 299 (4), 504–513.
62. Nichol JW; Koshy ST; Bae H; Hwang CM; Yamanlar S; Khademhosseini A, Cell-Laden Microengineered Gelatin Methacrylate Hydrogels. *Biomaterials* 2010, 31 (21), 5536–5544. [PubMed: 20417964]

63. Bonner JC; Badgett A; Osornio-Vargas AR; Hoffman M; Brody AR, Pdgf-Stimulated Fibroblast Proliferation Is Enhanced Synergistically by Receptor-Recognized Alpha 2-Macroglobulin. *J. Cell. Physiol* 1990, 145 (1), 1–8. [PubMed: 1698792]
64. Deuel TF; Kawahara RS; Mustoe TA; Pierce AF, Growth Factors and Wound Healing: Platelet-Derived Growth Factor as a Model Cytokine. *Annu. Rev. Med* 1991, 42, 567–584. [PubMed: 2035994]
65. Agren MS; Steenfos HH; Dabelsteen S; Hansen JB; Dabelsteen E, Proliferation and Mitogenic Response to Pdgf-Bb of Fibroblasts Isolated from Chronic Venous Leg Ulcers Is Ulcer-Age Dependent. *J. Invest. Dermatol* 1999, 112 (4), 463–469. [PubMed: 10201530]
66. Hori K; Sotozono C; Hamuro J; Yamasaki K; Kimura Y; Ozeki M; Tabata Y; Kinoshita S, Controlled-Release of Epidermal Growth Factor from Cationized Gelatin Hydrogel Enhances Corneal Epithelial Wound Healing. *J. Controlled Release* 2007, 118 (2), 169–176.
67. Li Z; Qu T; Ding C; Ma C; Sun H; Li S; Liu X, Injectable Gelatin Derivative Hydrogels with Sustained Vascular Endothelial Growth Factor Release for Induced Angiogenesis. *Acta Biomater* 2015, 13, 88–100. [PubMed: 25462840]
68. Vermonden T; Censi R; Hennink WE, Hydrogels for Protein Delivery. *Chem. Rev* 2012, 112 (5), 2853–2888. [PubMed: 22360637]
69. Lin C-C; Anseth KS, PEG Hydrogels for the Controlled Release of Biomolecules in Regenerative Medicine. *Pharm. Res* 2009, 26 (3), 631–643. [PubMed: 19089601]
70. Tabata Y; Ikada Y, Vascularization Effect of Basic Fibroblast Growth Factor Released from Gelatin Hydrogels with Different Biodegradabilities. *Biomaterials* 1999, 20 (22), 2169–2175. [PubMed: 10555085]
71. Thrailkill KM; Moreau CS; Cockrell G; Simpson P; Goel R; North P; Fowlkes JL; Bunn RC, Physiological Matrix Metalloproteinase Concentrations in Serum During Childhood and Adolescence, Using Luminex® Multiplex Technology. *Clin. Chem. Lab. Med* 2005, 43 (12), 1392–1399. [PubMed: 16309379]
72. Nguyen AH; McKinney J; Miller T; Bongiorno T; McDevitt TC, Gelatin Methacrylate Microspheres for Controlled Growth Factor Release. *Acta Biomater.* 2015, 13, 101–110. [PubMed: 25463489]

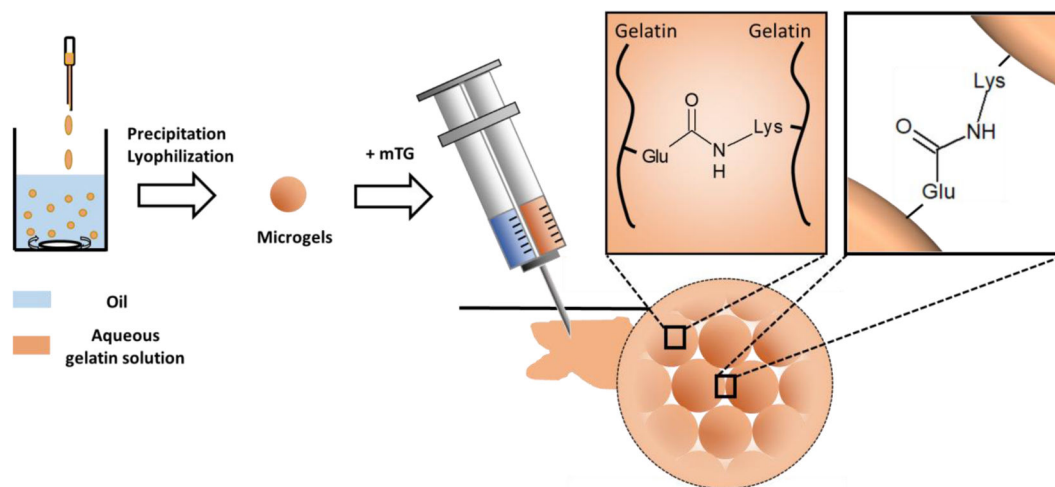


Figure 1: Schematic diagram of the microgel synthesis and the formation of porous hydrogel by crosslinking gelatin microgels with mTG. mTG crosslinks gelatins within the microgels and between microgels by creating amide bonds between glutamine (Glu) and lysine (Lys) residues.

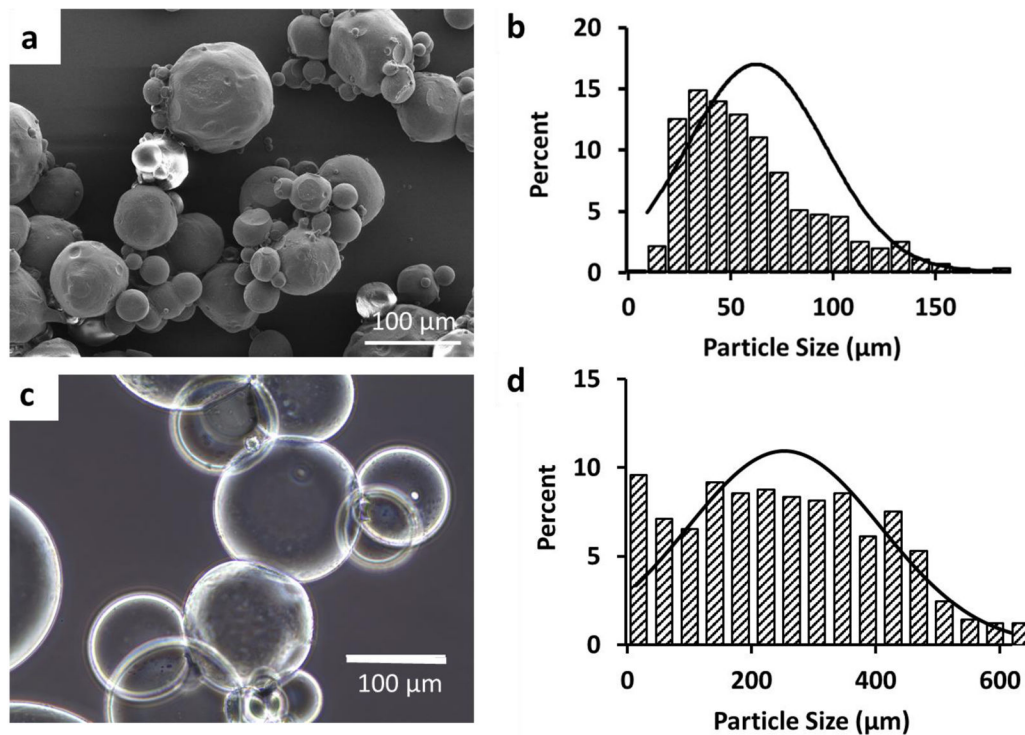


Figure 2: Gelatin microgels. a) SEM image of lyophilized (dry) microgels. b) Size distribution of the dry microgels. The average diameter of the dry microgels was $63\mu\text{m} (\pm 34\mu\text{m})$. c) Optical microscope image of the gelatin microgels after swelling in PBS. d) Size distribution of the microgels after swelling. The average diameter was $253\mu\text{m} (\pm 155\mu\text{m})$.

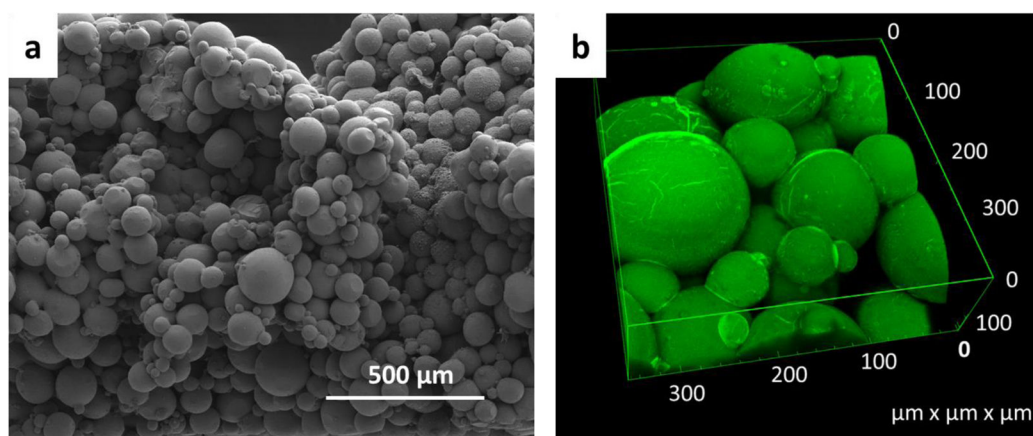


Figure 3: 3D structure of the porous hydrogel made of the crosslinked gelatin microgels. a) SEM image of the porous hydrogel after critical point drying. b) 3D rendition of the confocal microscope images of the porous hydrogel. Green fluorescence was obtained by the inclusion of FITC-BSA in the microgels.

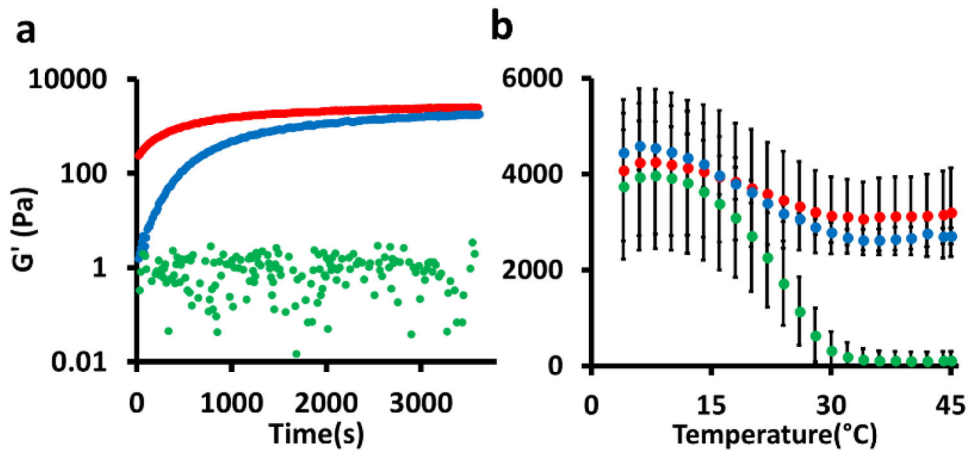


Figure 4: Rheological characterization of the hydrogels. a) Time sweep. b) Temperature sweep. Data are means with standard deviation ($n = 3$). Red: gelatin microgels + mTG (= macroporous hydrogel). Blue: gelatin solution + mTG (nonporous hydrogel). Green: gelatin microgels.

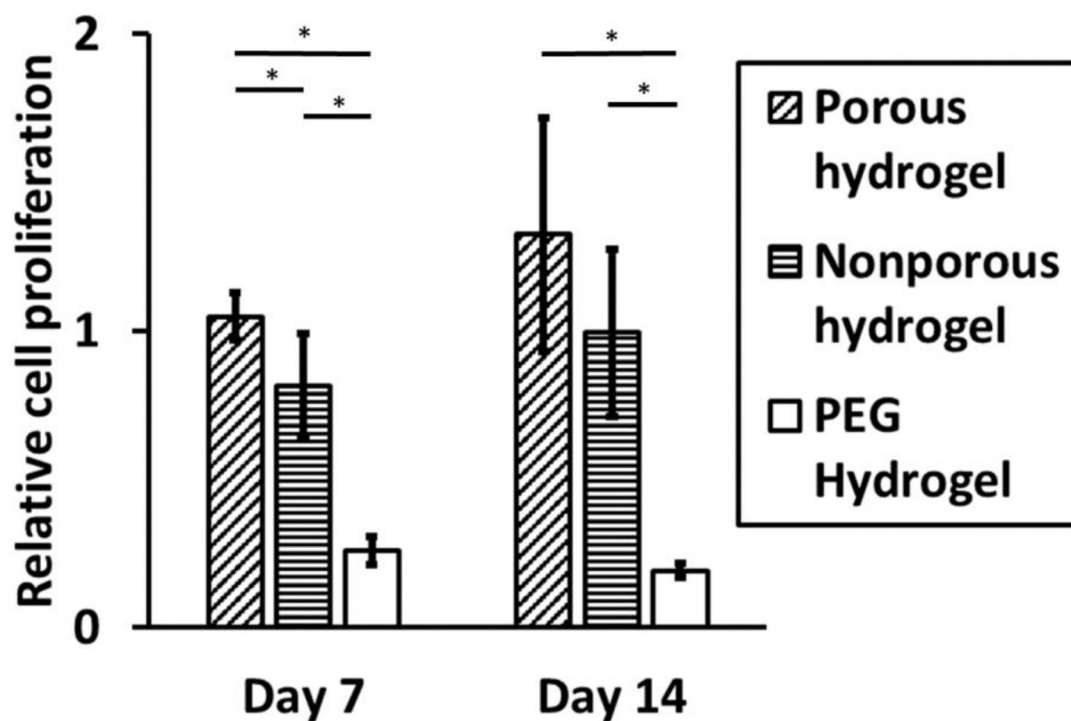


Figure 5: hDF proliferation on the hydrogels. Proliferation measured by alamarBlue assay was normalized to the proliferation on tissue culture polystyrene (TCPS). The data are means and standard deviation (n = 4, *p<0.05).

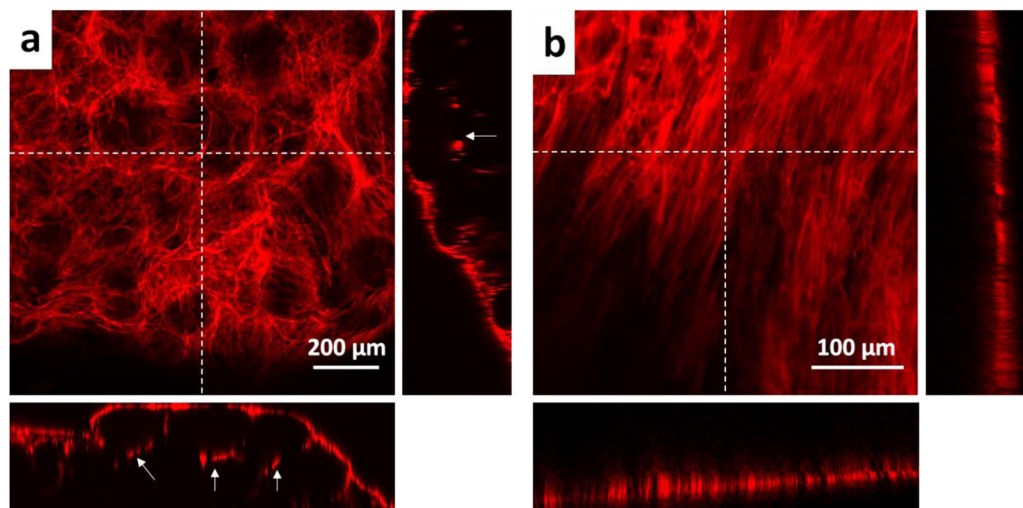


Figure 6: Maximum intensity projection of confocal microscope images a) porous hydrogel b) nonporous hydrogel. Actin cytoskeleton of hDFs was stained with actinRed555. The insets on the right and at the bottom of each image are the cross-sectional images corresponding to the vertical and horizontal dotted lines, respectively. The white arrows in the insets indicate the cells that grew underneath the microgels through the interstitial space.

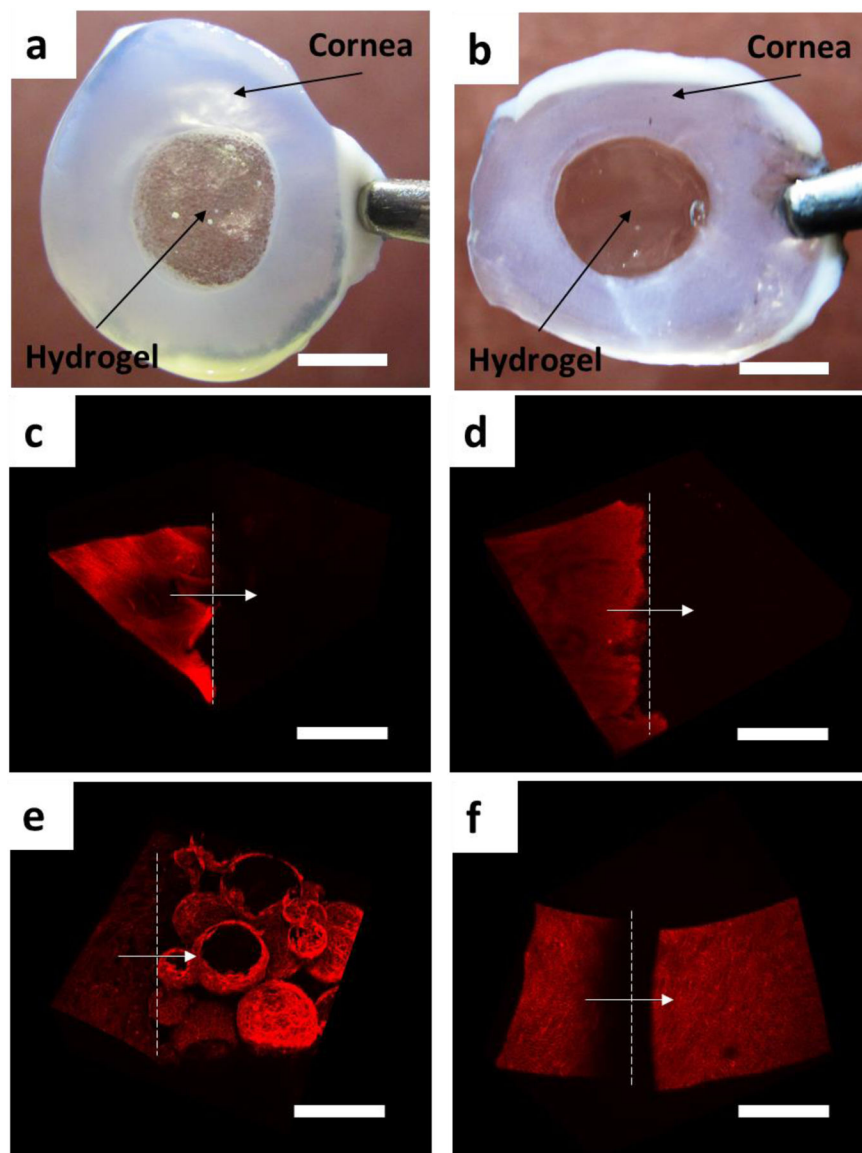


Figure 7: Tissue adhesion of the porous and nonporous gelatin hydrogels and cell migration. Porous (a) and nonporous (b) hydrogels were injected into a hole in an excised porcine cornea and were cultured for 14 days. The hydrogels stably adhered to the cornea tissues during that period. The cornea tissues turned opaque during the culture. (c, d) Confocal microscope images of the cornea-hydrogel interface of the porous (c) and nonporous (d) hydrogels on day 0. (e, f) day 14. Actin cytoskeleton was stained red using actinRed555. Dotted lines indicate the cornea-hydrogel interface with the arrows indicating the direction from cornea to hydrogel. The scale bar for (a, b) is 5 mm and for (c-f) is 200 μm .

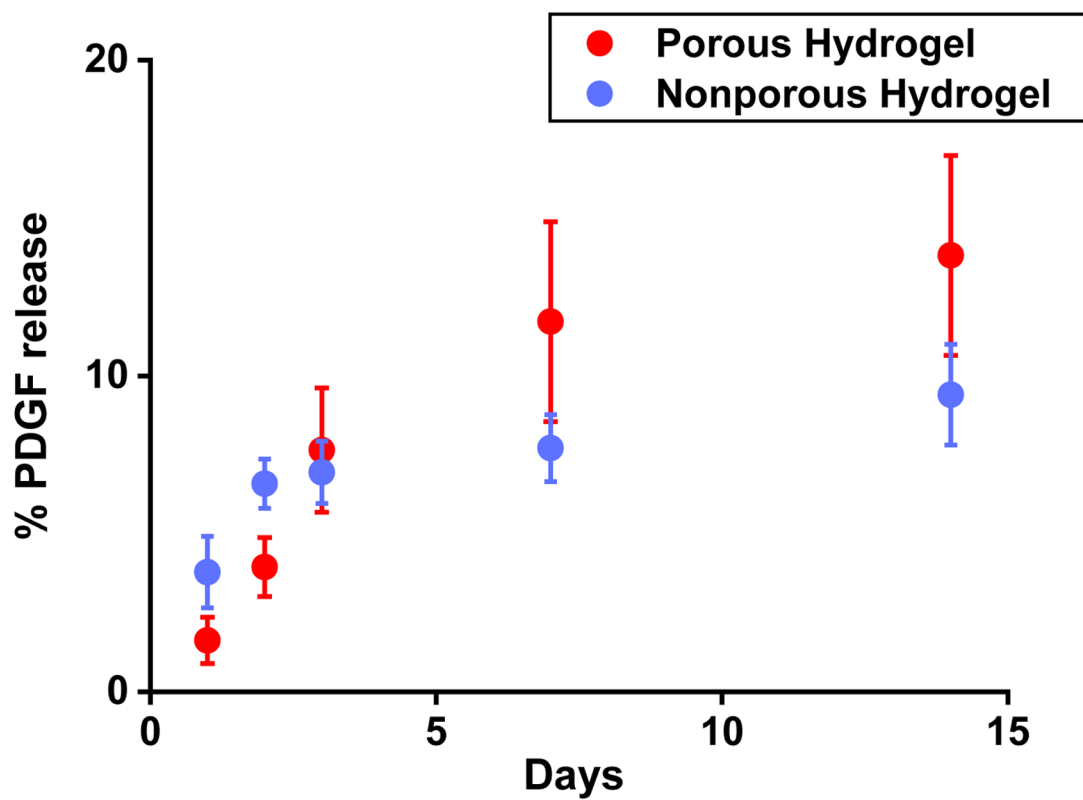


Figure 8: Cumulative release profile of PDGF from the hydrogels. The initial loading was 1.6 μg in 250 μL hydrogel. (n = 4)

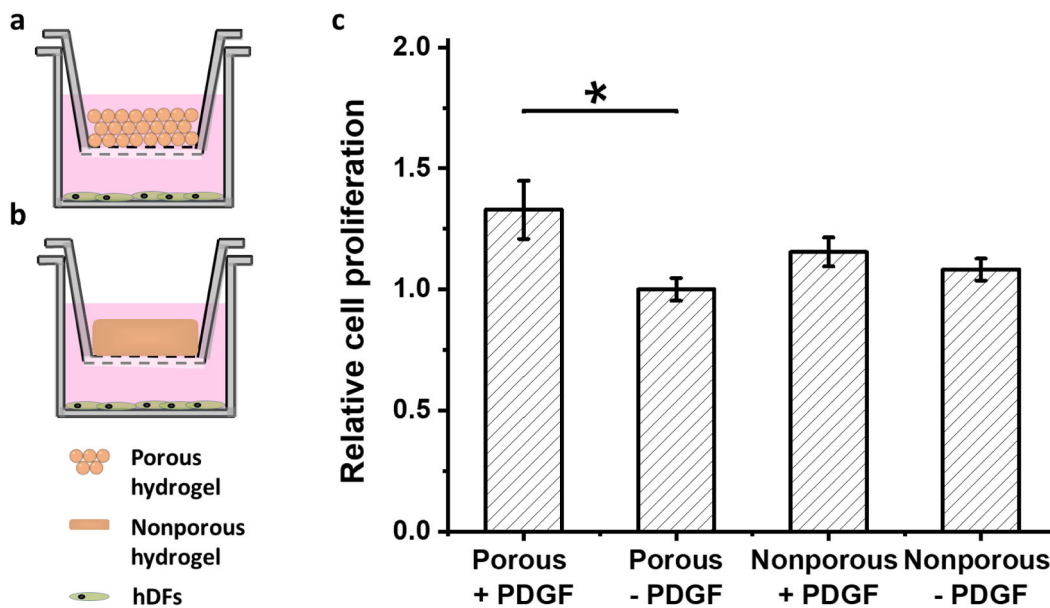


Figure 9: hDF proliferation with the controlled release of PDGF from the hydrogels. a) Schematic of the experimental design for (a) porous and (b) nonporous hydrogels. c) Relative proliferation at day 14. The proliferation was normalized to that of porous hydrogel without PDGF (n =4, *p<0.05)